Optics Letters

Femtosecond thulium fiber laser utilizing a gain-switched laser diode

Ibrahim H. Abughazaleh, Matthew D. Gerard, Panuwat Srisamran, Duanyang Xu, Yongmin Jung, and Lin Xu*

Optoelectronics Research Centre (ORC), University of Southampton, Southampton, SO17 1BJ, UK
**l.xu@soton.ac.uk*

Received 1 April 2025; revised 7 May 2025; accepted 12 May 2025; posted 13 May 2025; published 23 May 2025

We present an ultrafast thulium fiber laser based on nonlinear pulse compression of a gain-switched laser diode operating at 1.87 µm. Seeded by a 40-ps gain-switched laser diode (GSLD), thulium-doped fiber amplifiers (TDFA) are used to increase the pulse peak power, and a normal-dispersion highly nonlinear fiber (HNF) is employed to generate a positive chirp through self-phase modulation (SPM). A bandpass filter is introduced to remove the nonlinear chirp components induced by both SPM and gain switching. A two-stage compression process is employed to maximize pulse compression and suppress the pulse pedestal. The process begins with linear compression in a passive single-mode fiber, resulting in a 1.2-ps pulse duration, followed by soliton compression in a thulium fiber amplifier. This method produces pulses with an energy of 4.7 nJ and a near transform-limited compressed pulse width of 509 fs. The all-fiberized system shows great potential as a compact, affordable, and robust alternative to mode-locked lasers for ultrafast applications.

https://doi.org/10.1364/OL.564071

There is an increasing interest in the wavelength region that lies within the thulium emission band between 1.8 and 2 µm due to its numerous advantages in various fields such as medicine, material processing, spectroscopy, and remote sensing [1–4]. Thulium-doped fiber lasers (TDFLs) with ultrashort pulses are particularly of interest for their potential in mid-infrared generation and nonlinear optics where they serve as pump sources for nonlinear crystal-based optical parametric oscillators and supercontinuum generation in highly nonlinear fibers. In medical application, ultrafast TDFLs can be used as advanced light sources for multiphoton deep tissue imaging [1–4]. For the multiphoton imaging, the pulse requirements typically involve energies in the range of a few nanojoules and durations around a few hundred femtoseconds to produce detectable signals at depths ranging from several millimeters to sub-hundred micrometers below the surface [1,5].

Mode-locked fiber lasers have become the preferred method for generating femtosecond pulses in a compact form. However, achieving a stable single pulse operation requires precise control of dispersion, non-linearity, and polarization, making these systems sensitive to external factors such as temperature fluctuations and mechanical vibrations. These sensitivities affect their reliability and significantly limit their practical use in many real-world applications. To address this, polarization-maintaining fiber solutions have been developed to mitigate these changes [6–8]. Despite this, the repetition rates, and consequently the pulse parameters and potential applications, are determined by the length and detailed design of the mode-locked cavity, and in order to accommodate different use cases, it is often necessary to go through the time-consuming process of changing the cavity length and reoptimizing performance or constructing a new source completely.

In contrast, gain-switched laser diodes (GSLDs) offer a stable, compact, and readily available alternative to mode-locked lasers, providing greater operational flexibility in terms of repetition rate, pulse duration, and power. Their output and stability are electronically controlled, addressing many of the challenges associated with mode-locked lasers. However, constrained by the limits of modulation bandwidth and photon lifetime, typical laser diodes can only produce pulses with a minimum of tens-of-picosecond duration under gain-switched operation. To achieve shorter pulse durations, pulse compression is required, but it is challenging due to the narrow spectral bandwidth output and the nonlinear chirp associated with gain switching [9]. The nonlinear chirp occurs due to changes in the refractive index induced by the voltage applied during gain switching, which creates an up-chirp in the pulse followed by a down-chirp during relaxation [9]. These chirp changes create a temporal pedestal. To address this, saturable absorbers are used to clean up the chirp by filtering out the low-intensity pedestal, as demonstrated in the literature. For example, Fu *et.al*, utilized the intensity-dependent nature of self-phase modulation (SPM), followed by an offset filter to select the newly generated spectral component that corresponds to the main pulse peak, forming a Mamyshev regenerator system, which results in a pedestal-free output [10]. This approach is further enhanced by parabolic pulse evolution in the normal-dispersion regime at 1 µm in ytterbium-doped fibers, reducing the pulse width to 140 fs. However, the parabolic pulse evolution approach is not always suitable for shaping pulses at wavelengths

>1.3 μm within the anomalous dispersion regime of standard single-mode silica fibers (SMFs). Other techniques, such as nonlinear polarization rotation (NPR) or the use of a nonlinear amplifying loop mirror (NALM), have also been employed [11,12]. For example, Méchin et al., demonstrated a method that converted 14-ps pulses from a high-modulation-bandwidth (10 GHz) GSLD at 1.55 μm to a pedestal-free up-chirped pulse using a NALM, which were then linearly compressed to a duration of 2.5 ps using the anomalous dispersion of a length of SMF [12].

Generating sub-picosecond pulses from a GSLD in the thulium emission region faces great challenges due to the lack of high-modulation-bandwidth laser diodes and the anomalous dispersion from standard single-mode fibers at those wavelengths. Previous studies of TDFLs based on GSLDs all focused on long pulses, ranging from tens to hundreds of picoseconds [13,14].

In this paper, we demonstrate a novel method of nonlinear pulse compression for a GSLD at 1.87 μm. Coherent spectral broadening followed by linear pulse compression and soliton evolution is investigated, resulting in an all-fiberized TDFL system that effectively compresses pulses from the GSLD, reducing the 41-ps duration to an output of 509 fs. To the best of our knowledge, this represents the first demonstration of sub-ps pulse generation for a TDFL based on a GSLD.

Figure 1 presents the schematic of the laser system. A single-frequency laser diode (EP1854, Eblana Photonics) operating at a wavelength of 1875 nm was used as a seed source. Driven by an electrical pulse generator (8133A, Agilent), providing rectangular waveforms with 250 ps pulse width at a repetition rate of 32 MHz, the seed source was operated as a GSLD to generate optical pulses in the picosecond regime. The average power of the GSLD was less than 1 mW; therefore, two TDFAs were built to increase the power. TDFA1 comprised a 0.9-m-long thulium-doped fiber (TDF) that was core-pumped at 1565 nm with an in-house built erbium-doped fiber laser through a wave division multiplexer (WDM). The TDF was in-house fabricated using modified chemical vapor deposition (MCVD) and solution-doping techniques, which had a 10/100 μm core/cladding diameter, a 0.13 numerical aperture (NA), and a 0.2 wt.% Tm concentration. TDFA2 consisted of a 1.6-m-long TDF (LMA-TDF-25P/400-M, Coherent) that was cladding-pumped at 790 nm with a laser diode (e03, nLight) through a pump signal combiner. An isolator was placed after each of the TDFAs to prevent the unwanted backward-propagating light from damaging the seed laser. TDFA1 was configured to provide a high gain with a high optical to signal noise ratio (OSNR), and TDFA2 was designed to generate high output power. All the components within the amplifiers were directly spliced. The components between the amplifiers were connected through angled fiber patch cords. The pulses after the isolator were coupled into a 40-m-long HNF (UHNA4, Coherent) with normal dispersion at the laser wavelength to facilitate coherent spectral broadening. A fiber-packaged wavelength-tunable spectral bandpass filter (FOTF-020121131, Agiltron) was employed after the HNF to remove the spectral components with nonlinear chirps. A selection of SMF (SMF28e, Corning) with different lengths was used to characterize the linear pulse compression. TDFA3 was constructed and placed after the linear pulse compressor for the nonlinear pulse compression investigation. It comprised a 1.3-m-long in-house fabricated TDF that was core-pumped at 1560 nm with an erbium-doped fiber amplifier (Amonics, AEDFA-33-B-FA) through a WDM.

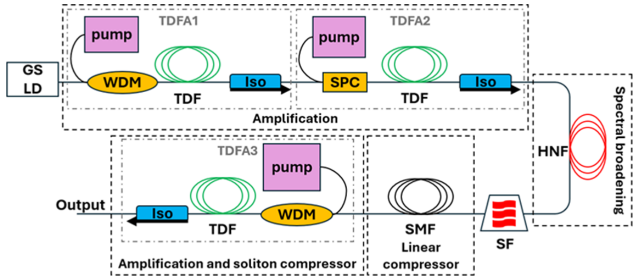

Fig. 1. Full detailed system schematics; inset functional schematics. GSLD, gain-switched laser diode; WDM, wave division multiplexer; TDF(A), thulium-doped fiber (amplifier); ISO, isolator; SPC, signal pump combiner; HNF, highly nonlinear fiber; SF, spectrum filter; SMF, single-mode fiber.

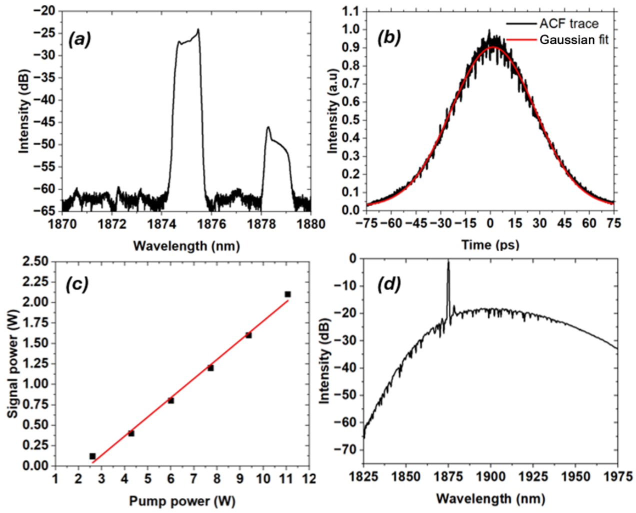

Fig. 2. (a) Laser diode output spectrum; (b) the autocorrelation trace (black) of the laser diode output and Gaussian fit (red); (c) the second stage amplifier output power against pump input power; (d) the second stage amplified spectrum.

With a set temperature of 23°C, the output spectrum of the GSLD exhibited a main peak at the central wavelength of 1875 nm with a 3-dB bandwidth of 1 nm, as shown in Fig. 2(a). A second peak, originating from the side mode oscillation, located at 1879 nm was observed on the spectrum, however, at a >20 dB lower intensity than the main peak. The average power from the GSLD was measured to be 12.3 μW and been increased to 40 mW from the TDFA1. The output pulses from the TDFA 1 were measured using an autocorrelator (PulseCheck nx150, APE), revealing a pulse width of 41 ps with a Gaussian-shaped assumption, as shown in Fig. 2(b). Figure 2(c) illustrates the power performance of TDFA2, showing a slope efficiency of 23% and a maximum output power of 2.1 W under a pump power of 11 W. Notable amplified spontaneous emission (ASE), at longer wavelengths in particular, was generated in TDFA2 at such a power level due to the cladding-pumped architecture; nevertheless, the amplified signal still exhibited a signal-to-noise ratio of over 20 dB and occupied 42.5% of the total power. Figure 3(b) shows the narrow signal spectrum at high resolution, revealing there is no significant nonlinear spectral distortion in the amplifier.

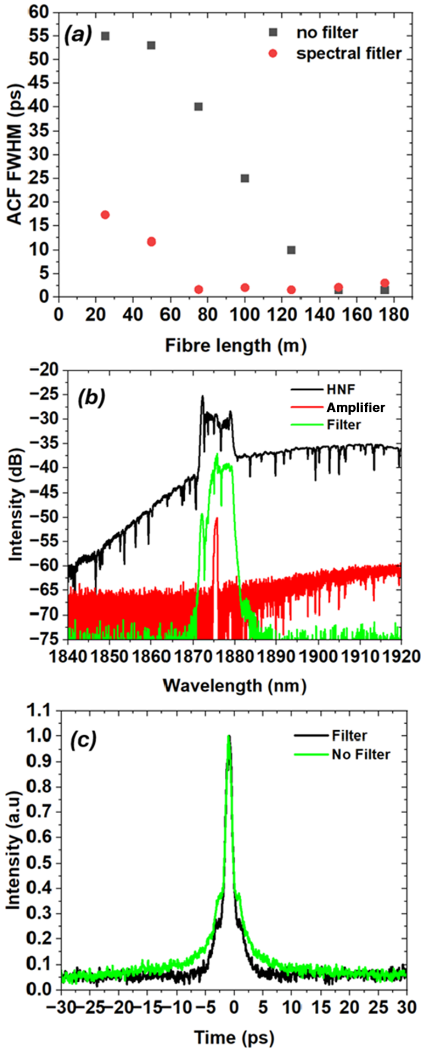

Fig. 3. (a) Change in the FWHM of the compressed pulse ACF with SMF fiber length with (red) and without (black) filter at the input; (b) the HNF input spectrum (red), the HNF output spectrum (black), and the filter output spectrum (green) offset by 25 dB; (c) the autocorrelation trace of the compressed broadened spectrum for 150 m of SMF without filter (green) and the minimum compressed pulse with filter at 125 m (black).

Spectral broadening, primarily driven by SPM, occurred during pulse propagation along the HNF, increasing the spectral bandwidth to 8.1 nm at the 10-dB level. Both the normal group velocity dispersion of the HNF and the SPM resulted in the pulses being positively chirped, which provides the opportunity to achieve pulse compression using typical (anomalously dispersive) SMFs. Before putting the spectral bandpass filter, 200-m-long SMFs were applied to characterize the linear pulse compression. It is worth noting that the input power into the SMF was attenuated to prevent undesired nonlinear effects within the SMF. Through the cut-back method, pulse compression with different fiber lengths was characterized, as shown in Fig. 3(a). Using the SMF with a length of 150 m, the pulses were effectively compressed to a duration of 1.5 ps. The measured autocorrelation trace of the compressed pulses is shown in Fig. 3(c), exhibiting a small pedestal that could be attributed to the nonlinear chirp component in the input pulses that was not compensated by the SMF. To reduce the nonlinear chirp component in the input pulse, a spectral bandpass filter was placed before the SMF. The central wavelength of the filter can be tuned around the laser wavelength, and the transmission bandwidth (3 dB) was ~3.6 nm. By carefully adjusting the central wavelength of the filter, improved linear pulse compression performance was obtained. The power after the filter was measured to be 51 mW. With a narrower input spectrum, the pulse width after the filter was measured to be 23 ps (ACF width), and the pulses could be effectively compressed through a much shorter length of SMF, as shown in Fig. 3(a). A minimum compressed pulse width of 1.2 ps was achieved by using a 125 m length of SMF. It is clear to see from Fig. 3(c) that the autocorrelation trace of the compressed pulse using the filter has a smaller pedestal, compared to that without using the filter. The main peak of the autocorrelation trace occupies 29% of the total area as opposed to 23% without the filter at the minimum compressed pulse duration. The pulse pedestal suppression was likely limited by the current filter bandwidth because the filter still transmitted some parts of the center and edge of the spectrum, which contain the nonlinear chirp generated from gain switching and SPM [15]. This could be overcome by using a filter with narrower bandwidths or by generating a wider spectrum in the HNF through increased fiber length or peak power. However, due to the positive chirps induced by the SPM and the normal dispersion of the HNF, the pulse temporally broadens, and the peak power reduces during the propagation. Therefore, the rate of spectral broadening exponentially decreases, making it inefficient in generating further spectral components. Nonetheless, great pulse compression performance and good-quality compressed pulses were successfully achieved by using the linear compression method, resulting in a significant pulse narrowing for the GSLD by a factor of 34.

The linearly compressed pulse was injected into the final TDFA to undergo nonlinear amplification and self-compression for further pulse narrowing. The amplifier showed a 23% slope efficiency and generated a maximum output power of 200 mW at 1 W of pump power, as shown in Fig. 4(a). The output spectrum of the amplifier broadened with the increase of the output power, as shown in Fig. 4(b), implying a nonlinear amplifier scheme. Pulse evolution and soliton formation were expected to happen within the amplifier, originating from the interplay between gain, anomalous dispersion, and SPM. The duration of the solitonic pulse is primarily determined by the fiber parameters and the pulse energy [16]. Autocorrelation measurements for the output pulses revealed pulse self-compression during the amplification. The pulses narrowed when the output power was increased up to 150 mW; however, further increase in the output power resulted in a slightly broader pulse with a higher pedestal shown on the autocorrelation trace, as presented in Fig. 4(c). At an output power of 150 mW, self-compressed pulses with high contrast and a pulse width of 509 fs were obtained. With a 10-dB bandwidth of 7.4 nm, the pulses exhibited a time–bandwidth product of (TBP) 0.321 that is close to the TBP value of 0.315 for a sech^2 pulse, confirming the soliton formation. The corresponding pulse energy and peak power are therefore 4.7 nJ and 8.52 kW, respectively.

In conclusion, we have successfully demonstrated a fully fiberized thulium-based laser system, seeded by a GSLD, capable of generating femtosecond pulses as an alternative to traditional mode-locked laser sources. The system incorporates a spectral filter to remove nonlinear chirp, effectively mitigating

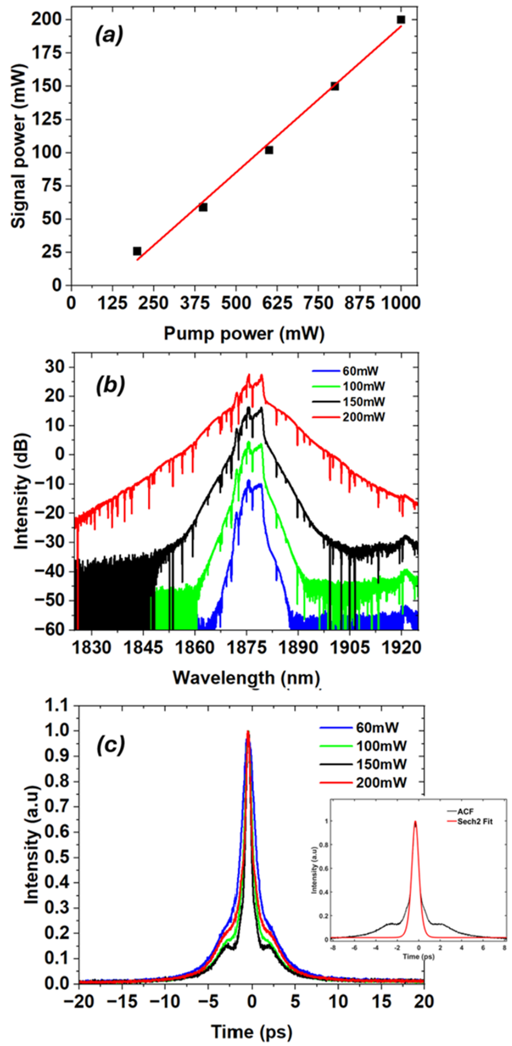

Fig. 4. (a) Final-stage amplifier characterization of signal power against pump power; (b) the amplified spectrum at different output power offset by 10 dB; (c) the autocorrelation at different output powers; inset: shorter scan range at 150 mW (black), $sech^2$ fit (red).

the temporal pedestal during linear compression. A final-stage amplifier was added to enhance the pulse intensity while forming a soliton, leading to further pulse compression to a near transform-limited duration of 509 fs. This represents a compression factor of approximately 80 from the initial 40-ps seed pulse, with over a twofold reduction in pulse duration compared to linear compression alone. The linear compression and spectral filtering stages are crucial for reducing the generated pedestal, by gradually controlling the pulse compression. Most notably, a significant difference between them is observed as a result of the peak-to-pedestal ratio. Future work should focus on employing a bandpass filter with a narrower range, coupled with precise fiber amplifier management, to ensure adiabatic pulse evolution and improved pedestal suppression. Overall, this system holds great promise as a compact, robust, and stable alternative to thulium-based mode-locked lasers for ultrafast pulse applications, including multiphoton microscopy.

Funding. Engineering and Physical Sciences Research Council (EP/T020997/2, EP/V038036/1, EP/P030181/1).

Acknowledgment. We would like to thank Prof. David Richardson at the ORC for useful discussion in this work.

Disclosures. The authors declare no conflicts of interest.

Data availability. Data can be accessed via [17].

REFERENCES

1. G. Sobon, A. Duzynska, M. Świniarski, *et al.*, Sci. Rep. **7**, 45491 (2017).
2. M. Michalska and J. Swiderski, Opt. Laser Technol. **118**, 121 (2019).
3. D. Klimentov, V. V. Dvoyrin, and I. T. Sorokina, IEEE Photonics Technol. Lett. **27**, 1609 (2015).
4. Y. W. Lee, J. Y. Chuang, C. C. Lin, *et al.*, Opt. Express **29**, 14682 (2021).
5. T. Srinivasan and M. Yildirim, Photonics **10**, 1307 (2023).
6. H. Hoogland, W. Hänsel, and R. Holzwarth, *2017 Conference on Lasers and Electro-Optics (CLEO)*, (2017), pp. 1–2.
7. M. Michalska, Ł. Gorajek, P. Grześ, *et al.*, *2019 Conference on Lasers and Electro-Optics Europe & European Quantum Electronics Conference (CLEO/Europe-EQEC),* (2019), p. 1.
8. Z. Łaszczych, M. Krakowski, and G. Soboń, Appl. Sci. **12**, 10613 (2022).
9. S. Chen, M. Yoshita, A. Sato, *et al.*, Opt. Express **21**, 10597 (2013).
10. W. Fu, L. G. Wright, and F. W. Wise, Optica **4**, 831 (2017).
11. N. Nishizawa and A. Murayama, Opt. Lett **32**, 3516 (2007).
12. D. Méchin, E. Le Cren, D. A. Reid, *et al.*, *2006 Conference on Lasers and Electro-Optics and 2006 Quantum Electronics and Laser Science Conference*, (2006), pp. 1–2.
13. A. M. Heidt, Z. Li, J. Sahu, *et al.*, *2013 Conference on Lasers and Electro-Optics Europe and International Quantum Electronics Conference CLEO EUROPE/IQEC*, (2013), Vvol. 38, pp. 1615–1617.
14. W. Yao, Z. Shao, C. Shen, *et al.*, Opt. Express **27**, 1276 (2019).
15. G. P. Agrawal, Nonlinear Fiber Opt. **1995**, 89 (1995).
16. T. Heuermann, C. Gaida, M. Gebhardt, *et al.*, *Laser Congress 2018 (ASSL), OSA Technical Digest* (Optica Publishing Group, 2018), p. AM5A.8.
17. I. H. Abughazaleh, M. D. Gerard, and P. Srisamran, “Code for ‘Femtosecond thulium fiber laser utilizing a gain-switched laser diode’,” Southampton (2025), https://doi.org/10.5258/SOTON/D3478.